# Propagation and Coupling Properties of Integrated Optical Waveguides—An Integral Equation Formulation

Spyridon J. Polychronopoulos and Nikolaos K. Uzunoglu, *Member, IEEE*

*Abstract*— **The propagation and coupling properties of integrated optical waveguides are analyzed by means of the electric field integral equation approach. The kernel of the integral equation is the Green's function of a two-layered medium. The Galerkin's method is then employed to solve the integral equation numerically. The set of basis and test functions consists of entire domain plane wave functions. Fast convergence and superior accuracy are the advantages of the chosen set of basis and test functions. The method is used to compute the propagation and coupling properties of several structures. Very good agreement is observed with previously published results. Field distributions of several coupled mode structures, such as the symmetrical and asymmetrical coupler are also investigated and presented. Finally, the same method is used to produce the field distribution of waveguides having more complex cross section like the trapezoidal waveguide.**

## I. Introduction

THE evolution of the integrated optical circuits technology has increased the need for accurate analysis and design methods of complex dielectric structures. Approximate methods can be valuable tools when high accuracy is not required. Two examples of such methods are Marcatili's method [1] and the effective index method [2]–[4]. When high precision results are necessary, it is crucial to use more sophisticated numerical methods.

A paper that reviews such methods, until 1985, has been published by Saad [5]. The most popular methods are the mode matching [6]–[12], the finite element [13]–[19], the finite difference [20], [21] and the methods based on integral equations [22]–[29]. In order to discretise the continuous spectrum and make the modes countable, some of the mode matching techniques introduce fictitious electric or magnetic walls [7]–[9]. The finite difference and finite element methods are versatile regarding the shape of the waveguiding structure but usually require the definition of boundary walls on which "artificial" absorbing boundary conditions are implemented. They also need a large number of unknowns. In the earlier finite element methods the presence of spurious modes was a serious drawback [13]–[17]. More recent formulations that use the $H_x - H_y$ or $E_x - E_y$ formulation eliminate this problem [18]–[19]. Finally, the integral equation methods can be divided into the domain [22]–[28] and the surface integral techniques [29].

The integral equation approach has the advantage that it rigorously takes into account the radiation conditions, of the open structure, and therefore it is not necessary to implement absorbing boundary conditions. The domain integral method considers the unknown field inside the waveguides as an equivalent polarization source. The electric field inside the waveguides satisfies the Fredholm equation of the second kind. The kernel of the integral equation is the Green's dyadic function of the embedding. This approach inherently predicts all the possible properties of the embedding like radiation, leakage effects [22], [23], [25], anisotropy, stratification [24]–[28], etc., through Green's function.

In this paper, an electric field integral equation method for modeling waveguides in a two-layered isotropic medium is presented. The method is applicable for any number of parallel waveguides arbitrarily positioned inside and/or outside the substrate. The cross section of the waveguides is considered to be rectangular. In order to transform the system of integral equations to a linear matrix system the method of moments has been employed. A distinct difference of the present method is the set of basis and test functions that is used to describe the unknown field. The usual approach is to apply the collocation method (point matching) or a similar subdomain method [22], [24]–[27]. The collocation method is versatile and easy to implement but it presents two serious drawbacks. The first, which is common to all subdomain methods, is the large number of unknowns and therefore the large required memory, CPU time and possible numerical instabilities. The second problem is the creation of fictitious charges and currents on the boundaries of the subdomains due to the discontinuous variation of the electromagnetic field. Both problems can be sufficiently confronted if one uses entire domain functions to describe the field. In the present approach the field inside each waveguide is described as superposition of plane waves. Since this is a very "natural" description, the method converges rapidly and the size of the system's matrix is relatively small. Therefore economy in computer memory and CPU time is achieved. Propagation constants, field distributions and coupling properties are numerically computed. Convergence is checked by successively increasing the number of test functions. Since there are no theoretical constraints about the

Manuscript received September 17, 1993; revised January 17, 1996.

The authors are with the Department of Electrical and Computers Engineering, National Technical University of Athens, Athens 10682, Greece.

Publisher Item Identifier S 0018-9480(96)03020-7.

number, the size and the distance between the waveguides, it is feasible, using the same code, to model simple waveguides, symmetrical or asymmetrical couplers and waveguides having more complicated cross section.

The theoretical analysis of the approach is presented in Section II. The basic steps are the formulation of the system of integral equations, the calculation of Green's dyadic function and the description of the electric field inside each waveguide. In Section III the numerical solution is presented, i.e., Galerkin's method as applied to the specific problem. Section IV is devoted to the presentation of the numerical results. Finally, conclusions are given in Section V.

## II. Theoretical Analysis

The geometry of the analyzed structure is shown in Fig. 1. The embedding consists of a two-layered medium, namely the substrate (region $V_1$) and the cover (region $V_0$). Inside the embedding there are $N$ waveguides (regions $V_{2,i}, i = 1, 2, \cdots, N$) of rectangular cross section. The structure is non symmetrical and the distance between the boundaries of the waveguides can vary from zero to infinity. The materials of the regions $V_0, V_1, V_2$ are considered homogeneous, isotropic and lossless with real refractive indexes $n_0, n_1, n_2$. The harmonic time factor is assumed to be $\exp(-j\omega t)$ and will be suppressed throughout this analysis. In the absence of incident field (excitation) the electric field $\underline{E}(\underline{r})$ (the underbar denotes vectors) satisfies the homogeneous Fredholm equation of the second kind

$$\underline{E}(\underline{r}) = \iiint_{V_\infty} \overline{\underline{G}}(\underline{r}, \underline{r}') \cdot (k^2(\underline{r}') - k_n^2(\underline{r}'))\underline{E}(\underline{r}')\, d\underline{r}', \quad \underline{r} \in V_\infty \tag{1}$$

$$k(\underline{r}') = \frac{2\pi}{\lambda_0} \cdot \begin{cases} n_0, & \underline{r}' \in V_0 \\ n_1, & \underline{r}' \in V_1 \\ n_2, & \underline{r}' \in V_2 \end{cases} \tag{2}$$

$$k_n(\underline{r}') = \frac{2\pi}{\lambda_0} \cdot \begin{cases} n_0, & y' > 0 \\ n_1, & y' \le 0 \end{cases} \tag{3}$$

where $\lambda_0$ is the wavelength in vacuum and $\overline{\underline{G}}(\underline{r}, \underline{r}')$ (the doublebar denotes dyadics) is the electric Green's dyadic function of the embedding. In the space of generalized functions the singularities of the source point are inherently contained in the electric Green's dyadic function [30], [31].

The next step of the analysis is to write the Green's dyadic function. Since the waveguides can be placed everywhere, then the vertical coordinate of $\underline{r}'$ can vary from minus to plus infinity ($-\infty < y' < \infty$). In the literature the usual expressions for Green's function assume that the source point is located either in the substrate or in the cover. In this analysis it is advantageous to derive a unified expression for Green's function that will describe the impulse response of the system when $-\infty < y' < \infty$. It is first assumed, that the source point is located inside the substrate ($y' < 0$), and then the spectral representation of Green's function is calculated. Next the source is positioned in the cover ($y' > 0$). Finally, a unified

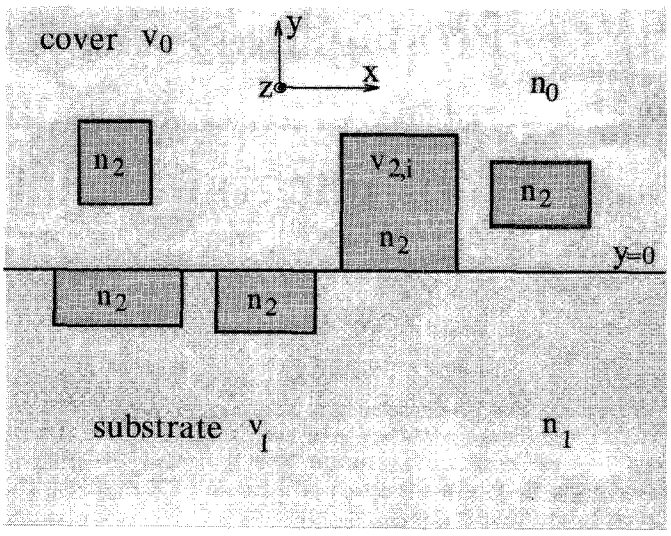


Fig. 1. General structure for integral equation analysis.

expression for $-\infty < y' < \infty$ is derived

$$\overline{\underline{G}}(\underline{r}, \underline{r}') = \begin{cases} \overline{\underline{G}}_0(\underline{r}, \underline{r}') + \overline{\underline{G}}_1(\underline{r}, \underline{r}'), & y \cdot y' \ge 0 \\ \overline{\underline{G}}_2(\underline{r}, \underline{r}'), & y \cdot y' < 0 \end{cases} \quad -\infty < y' < \infty \tag{4}$$

where $\overline{\underline{G}}_0(\underline{r}, \underline{r}')$ is the primary part $\overline{\underline{G}}_1(\underline{r}, \underline{r}'), \overline{\underline{G}}_2(\underline{r}, \underline{r}')$ and are the secondary parts and can be thought of as the reflected and transmitted parts due to the boundary at $y = 0$.

The spectral representation of $\overline{\underline{G}}_0(\underline{r}, \underline{r}')$ is well known and can be written as [32]

$$\begin{aligned} \overline{\underline{G}}_0(\underline{r}, \underline{r}') &= \frac{1}{8\pi^3} \int_{-\infty}^{+\infty} \int_{\substack{-\infty \\ \epsilon \to 0^+}}^{+\infty} \int_{-\infty}^{+\infty} (\overline{\underline{1}} - k_n^{-2} \underline{h}\underline{h}) \\ &\quad \cdot \frac{e^{j\underline{h} \cdot (\underline{r} - \underline{r}')}}{h^2 - k_n^2 - j\epsilon} d\underline{h} \\ &= \frac{k_n^{-2}}{8\pi^2} \int_{-\infty}^{+\infty} \int_{\substack{-\infty \\ \epsilon \to 0^+}}^{+\infty} e^{j\underline{h}_0 \cdot (\underline{r} - \underline{r}')} \overline{\underline{g}}_0(h_x, h_z, y', (y - y')) \\ &\quad dh_x\, dh_z - k_n^{-2} \delta(\underline{r} - \underline{r}') \hat{y}\hat{y} \end{aligned} \tag{5}$$

$$\overline{\underline{g}}_0(h_x, h_z, y', (y - y')) = \frac{1}{\mu}(\overline{\underline{1}} k_n^2 - \underline{h}_0 \underline{h}_0). \tag{6}$$

The $\delta(\underline{r} - \underline{r}')$ singular term arises naturally after performing the $\int_{-\infty}^{+\infty} dh_y$ Fourier integration [35]. By doing so the principal volume of integration becomes the "slice" $y = y'$ or its equivalent "disc shaped pillbox" [33]–[35].

The vector $\underline{h}_0$ is found to be

$$\underline{h}_0(y', (y - y')) = h_x \hat{x} + h_z \hat{z} + h_{y0} \hat{y},$$

$$h_{y0}(y', (y - y')) = jsu \tag{7}$$

$$s(y - y') = \operatorname{sign}(y - y') \tag{8}$$

$$\mu(h_x, h_z, y') = \sqrt{|k_n^2 - h_x^2 - h_z^2|} \cdot \begin{cases} (\epsilon - j), & k_n^2 > h_x^2 + h_z^2 \\ (1 - j\epsilon), & k_n^2 < h_x^2 + h_z^2, \end{cases} \quad \epsilon \to 0^+. \tag{9}$$

The exponential variable $\mu_{0,1}$ has been evaluated using the limiting absorption principle, i.e., assuming that the materials have infinitesimal small losses. Then the radiation conditions are automatically satisfied [36]. The infinitesimal losses are introduced through the $\epsilon$ term which from now on, for brevity, will be omitted.

Similarly, the unified expressions for $\overline{G}_1, \overline{G}_2$ are

$$\overline{G}_1(\underline{r},\underline{r}') = \frac{k_n^{-2}}{8\pi^2}\int_{-\infty}^{+\infty}\int_{-\infty}^{+\infty} e^{j\underline{h}_1\cdot\underline{r}-jh_x x'-jh_z z'-s_0\mu y'} \cdot \overline{g}_1(h_x,h_z,y')\,dh_x\,dh_z \tag{10}$$

$$\overline{G}_2(\underline{r},\underline{r}') = \frac{k_n^{-2}}{8\pi^2}\int_{-\infty}^{+\infty}\int_{-\infty}^{+\infty} e^{j\underline{h}_2\cdot\underline{r}-jh_x x'-jh_z z'-s_0\mu y'} \cdot \overline{g}_2(h_x,h_z,y')\,dh_x\,dh_z. \tag{11}$$

The vectors $\underline{h}_1, \underline{h}_2$ are given by

$$\underline{h}_1(y') = h_x\hat{x} + h_z\hat{z} + h_{y1}\hat{y}, \quad h_{y1}(y') = js_0\mu \tag{12}$$

$$\underline{h}_2(y') = h_x\hat{x} + h_z\hat{z} + h_{y2}\hat{y}, \quad h_{y2}(y') = -js_0\mu - \tag{13}$$

$$s_0(y') = \operatorname{sign}(y') \tag{14}$$

$$k_n'(\underline{r}') = \frac{2\pi}{\lambda_0}\cdot\begin{cases} n_0, & y'\le 0 \\ n_1, & y'>0 \end{cases} \tag{15}$$

$$u'(h_x,h_z,y') = \sqrt{|k_n'^2 - h_x^2 - h_z^2|} \cdot\begin{cases} (\epsilon - j), & k_n'^2 > h_x^2+h_z^2 \\ (1-j\epsilon), & k_n'^2 < h_x^2+h_z^2, \end{cases} \quad \epsilon\to 0^+. \tag{16}$$

The unknown dyadic functions $\overline{g}_1, \overline{g}_2$ are found satisfying the boundary conditions at $y = 0$ (Appendix A).

The following step is to determine the system of integral equations. Since we are interested only in the propagating modes, the electric field inside the $i$'th waveguide can be assumed to have the following form

$$\underline{E}_i(\underline{r}) = e^{j\beta z}\underline{e}_i(x,y), \quad \underline{r}\in V_{2,i}, \quad \beta>0, \quad \beta\text{: propagation constant} \tag{17}$$

and its spectral representation is

$$\underline{E}_i(\underline{r}) = e^{j\beta z}\int_{-\infty}^{+\infty}\int_{-\infty}^{+\infty}\underline{c}_i(k_x,k_y)e^{jk_x x+jk_y y}\,dk_x\,dk_y, \quad \underline{r}\in V_{2,i} \tag{18}$$

where $\underline{c}_i(k_x,k_y)$ is the Fourier transform of the electric field.

It is simple to verify that the above spectral representation satisfies the following wave equation:

$$(\nabla^2 + k_2^2)\underline{E}_i(\underline{r}) = 0$$

when

$$k_x^2 + k_y^2 = k_2^2 - \beta^2$$

which suggests writing $k_x, k_y$ as

$$k_x(\phi_k) = \sqrt{k_2^2-\beta^2}\cos(\phi_k),$$
$$k_y(\phi_k) = \sqrt{k_2^2-\beta^2}\sin(\phi_k),$$
$$k_2 = \frac{2\pi}{\lambda_0}n_2, \qquad 0\le\phi_k<2\pi$$

then the double Fourier transform (18) reduces to a single one

$$\underline{E}_i(\underline{r}) = e^{j\beta z}\int_0^{2\pi}\underline{c}_i(\phi_k)e^{jk_x x+jk_y y}\,d\phi_k, \qquad \underline{r}\in V_{2,i}. \tag{19}$$

We can now form the system. Equation (1) can be written as

$$\begin{aligned}\underline{E}_i(\underline{r}) &= \sum_{m=1}^{N}\iiint_{V_{2,m}}\overline{G}(\underline{r},\underline{r}')\cdot(k^2(\underline{r}') - k_n^2(\underline{r}'))\underline{E}_m(\underline{r}')\,d\underline{r}' \\ &= \sum_m (k_2^2 - k_n^2(m))\iiint_{V_{2,m}}(\overline{G}_0(\underline{r},\underline{r}') + \overline{G}_1(\underline{r},\underline{r}')) \cdot\underline{E}_m(\underline{r}')\,d\underline{r}' + \sum_m(k_2^2-k_n^2(m))\iiint_{V_{2,m}}\overline{G}_2(\underline{r},\underline{r}') \cdot\underline{E}_m(\underline{r}')\,d\underline{r}'\end{aligned}$$

$$k_n(m) = \frac{2\pi}{\lambda_0}\cdot\begin{cases} n_0, & \text{if } V_{2,m} \text{ is in the cover} \\ n_1, & \text{if } V_{2,m} \text{ is in the substrate.}\end{cases} \tag{20}$$

In the first summation, index $m$ is allowed to take only the values of the indexes of those waveguides that are in the same region with the $i$'th waveguide, while in the second summation $m$ takes the remaining values. Substituting $\overline{G}_0(\underline{r},\underline{r}')$ from ((5), (6)), $\overline{G}_1(\underline{r},\underline{r}')$ from (10), $\overline{G}_2(\underline{r},\underline{r}')$ from (11), $\underline{E}_i(\underline{r})$ and $\underline{E}_m(\underline{r})$ from (19) into (20) and performing the double integration

$$\int_{-\infty}^{+\infty}dh_z\int_{-\infty}^{+\infty}dz'\,e^{j(\beta-h_z)z'}F(h_z) = 2\pi F(\beta) \tag{21}$$

it is found

$$\sum_m\left\{\overline{L}_{im}^A[\cdot\underline{e}_m(x',y')](x,y) - \delta_{im}\left[\overline{\underline{1}} + \frac{k_2^2-k_n^2(m)}{k_n^2(m)}\hat{y}\hat{y}\right]\cdot\underline{e}_m(x,y)\right\} + \sum_m\{\overline{L}_{im}^B[\cdot\underline{e}_m(x',y')](x,y)\} = 0 \tag{22}$$

where the symbols $\overline{L}_{im}^A[\ ], \overline{L}_{im}^B[\ ]$ have been used for the following integral operators:

$$\begin{aligned}\overline{L}_{im}^A[\ ] = \frac{k_2^2-k_n^2(m)}{4\pi k_n^2(m)}\int_{-\infty}^{+\infty}dh_x\iint_{S_m}dx'\,dy'\{&e^{jh_x(x-x')} \cdot[e^{-s\mu(y-y')}\overline{g}_0(h_x,\beta,y',(y-y')) \\ &+ e^{-s_0\mu(y+y')}\overline{g}_1(h_x,\beta,y')[\ ]\}, \qquad \underline{r}\in S_i\end{aligned} \tag{23a}$$

$$\overline{L}_{im}^B[\ ] = \frac{k_2^2-k_n^2(m)}{4\pi k_n^2(m)}\int_{-\infty}^{+\infty}dh_x\iint_{S_m}dx'\,dy'\,e^{jh_x(x-x')} \cdot e^{s_0(\mu' y-\mu y')}\overline{g}_2(h_x,\beta,y')[\ ], \qquad \underline{r}\in S_i \tag{23b}$$

$\delta_{im}$ denotes Kronecker's symbol

$$\delta_{im} = \begin{cases} 1, & i=m \\ 0, & i\ne m\end{cases} \tag{24}$$

and $S_i$ denotes the cross section of the $i$'th waveguide.

Writing (22) for $i = 1, 2, \cdots, N$ a system of integral equations containing $N$ unknowns, i.e., the field vectors $e_i(x,y)$ is obtained. In the next section Galerkin's method is applied to numerically solve the above system.

## III. Numerical Solution

To numerically solve the system of integral equations Galerkin's method is employed. To achieve this, a set of basis (test) functions for the description of the unknown field, inside each waveguide, is chosen. Since description (19) satisfies the wave equation it is reasonable that an approximate form of (19) will be advantageous. To this end the integral representation (19) of the unknown field in the $m$th waveguide is discretized as

$$\underline{e}_m(x',y') = \sum_{l'=1}^{L} \underline{c}_{ml'} e^{jk'_x x' + jk'_y y'} \tag{25a}$$

$$\underline{c}_{ml'} = \underline{c}_m(\phi_k(l')), \qquad l' = 1,2,\cdots L \tag{25b}$$

$$k'_x(l') = \sqrt{k_2^2 - \beta^2}\cos(\phi_k(l'), \qquad l' = 1,2,\cdots,L$$
$$k'_y(l') = \sqrt{k_2^2 - \beta^2}\sin(\phi_k(l')), \qquad l' = 1,2,\cdots,L \tag{25c}$$

where $\phi_k(l')$ is the discrete spectral angle

$$\phi_k(l') = \frac{2\pi}{L}(l'-1), \qquad l' = 1,2,\cdots,L. \tag{26}$$

Therefore the set of basis functions consists of the plane waves

$$f_{l'}(x',y') = e^{jk'_x x' + jk'_y y'}, \qquad l' = 1,2,\cdots,L. \tag{27}$$

In order to apply Galerkin's method we choose as a set of weighting functions

$$f_l(x,y) = e^{jk_x x + jk_y y}, \qquad l = 1,2,\cdots L \tag{28a}$$

$$k_x(l) = \sqrt{k_2^2 - \beta^2}\cos(\phi_k(l)), \qquad l = 1,2,\cdots,L$$
$$k_y(l) = \sqrt{k_2^2 - \beta^2}\sin(\phi_k(l)), \qquad l = 1,2,\cdots,L. \tag{28b}$$

Substitution of (25) into (22) produces

$$\sum_{l'=1}^{L}\left\{\sum_m \left\{\underline{\overline{L}}^A_{lm}[f_{l'}(x',y')](x,y) - \delta_{lm}\left[\underline{\underline{1}} + \frac{k_2^2 - k_n^2(m)}{k_n^2(m)}\hat{y}\hat{y}\right]\right.\right.$$
$$\left.\left. \cdot\, f_{l'}(x,y)\right\} + \sum_m \{\underline{\overline{L}}^B_{lm}[f_{l'}(x',y')](x,y)\}\right\} \cdot \underline{c}_{ml'} = 0 \tag{29}$$

Finally, the method of moments [37], [38] is applied to the above equation, using as a weighting function the one given by (28)

$$\sum_{l'=1}^{L}\left\{\sum_m \left\{\langle \underline{\overline{L}}^A_{lm}[f_{l'}(x',y')](x,y), f_l(x,y)\rangle \right.\right.$$
$$\left. - \delta_{lm}\left[\underline{\underline{1}} + \frac{k_2^2 - k_n^2(m)}{k_n^2(m)}\hat{y}\hat{y}\right]\langle f_{l'}(x,y), f_l(x,y)\rangle\right\}$$
$$\left. + \sum_m \{\langle \underline{\overline{L}}^B_{lm}[f_{l'}(x',y')](x,y), f_l(x,y)\rangle\}\right\} \cdot \underline{c}_{ml'} = 0. \tag{30}$$

The symbol $\langle\cdot,\cdot\rangle$ denotes the inner product of two scalar functions, e.g.,

$$\langle \underline{\overline{L}}^{A,B}_{lm}[f_{l'}(x',y')](x,y), f_l(x,y)\rangle = \iint_{S_i} \underline{\overline{L}}^{A,B}_{lm}[f_{l'}(x',y')](x,y) f_l^*(x,y)\, dx\, dy \tag{31}$$

where $f^*$ is the complex conjugate of $f$.

Until now the analysis is valid for arbitrarily shaped waveguides. If the cross section is rectangular, the double spatial integration $\int\int_{S_i} dx\, dy \int\int_{S_m} dx'\, dy'$ can be performed analytically (Appendix B). The infinite Fourier integrals that remain are truncated and computed numerically using a multisegment quadratic Gaussian method of twelve points [39]. Convergence is checked by successively increasing the number of segments and choosing a sufficiently large domain of integration.

Writing (30) for $i = 1,2,\cdots N, l = 1,2,\cdots,L$ a linear homogeneous system of $N \cdot L$ vector equations is formed. The unknowns are the propagation constant and the vectors $c_{ml'}, m = 1,2\cdots,N, l' = 1,2,\cdots,L$. In order to find the eigenvectors $c_{ml'}$ of a surface mode one has to search for the roots of the determinant of the matrix of the system, i.e., $\beta$: $\det[A](\beta) = 0$, where $[A](\beta)$ is the matrix of the system and $\beta$ is the propagation constant of the surface mode. Once the vectors $\underline{c}_{ml'}$ have been found the modal distribution in the $m$'th waveguide is computed using (25).

## IV. Numerical Results

A FORTRAN program that implements the previous full vectorial analysis has been developed. Input data of this program are the geometrical parameters of the structure, the refractive indexes, and the wavelength in free space. The program calculates the propagation constants and the modal distributions of the existing surface modes. For the presentation of the results the following annotations [1] have been used:

Symbol $v$ denotes the normalized frequency

$$v = \frac{k_0 t}{\pi}\sqrt{n_2^2 - n_1^2} \tag{32}$$

where $t$ is a typical dimension of the waveguides. Symbol $b$ denotes the normalized propagation constant

$$b = \frac{(\beta/k_0)^2 - n_1^2}{n_2^2 - n_1^2}, \qquad 0 < b < 1. \tag{33}$$

The first example considered is the channel waveguide shown in Fig. 2. In the diagram of Fig. 2 are plotted the dispersion curves of the $E_{11}^y$ and $E_{21}^y$ modes. For comparison results of the finite element method [18], finite difference method [21] and effective index method have been included.

In Fig. 3 is shown the convergence of the propagation constant of the $E_{11}^y$ mode versus the number of test functions for $v = 1$. Sufficient convergence (eventhough nonmonotonic)

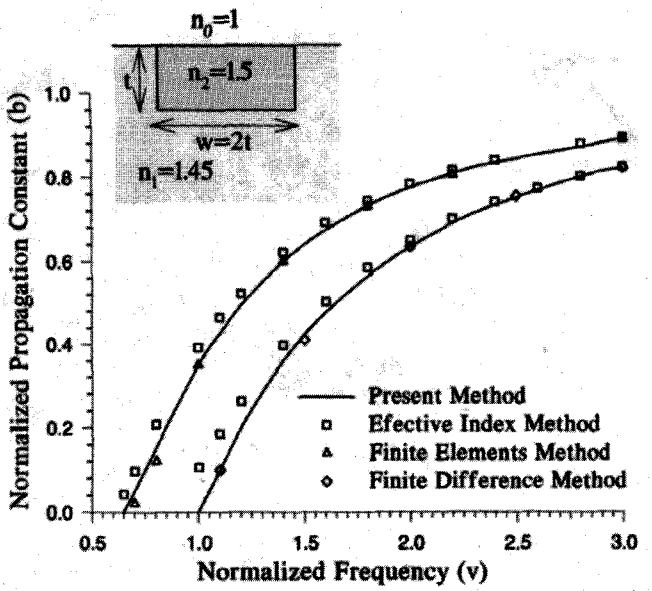


Fig. 2. Normalized propagation constant versus normalized frequency of a channel waveguide. $n_0 = 1, n_1 = 1.45, n_2 = 1.5, w/t = 2$.

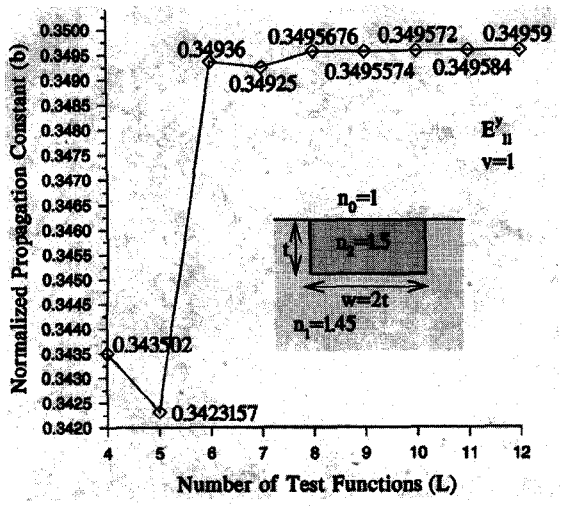


Fig. 3. Convergence of the normalized propagation constant of the $E_{11}^y$ mode. Normalized frequency $v = 1$.

is achieved using six or more test functions. If one uses nine test functions the total scalar unknowns are $3 \times 9 = 27$ and the evaluation of the system's matrix requires the evaluation of $27^2$ elements. Remarkable property of the system's matrix is its high redundancy. In this example the redundancy is 70% which means 70% reduction of the execution time. Using a PC-486 (DX4/100 MHz), four seconds are sufficient to calculate the determinant of the matrix.

Fig. 4 depicts the power distribution of the $E_{11}^y$ mode, i.e., the main transverse component $|E_y|^2$ (up), the longitudinal component $|E_z|^2$ (middle) and the weak component $|E_x|^2$ (down). In a similar fashion, Fig. 5 shows the power distribution of the $E_{21}^y$ mode. These plots are based on equation (25) using nine test function ($L = 9, N = 1$). Baken *et al.* [26] using the collocation method to solve a similar integral equation problem, have reported that for a grid of 72×36 nodes a result could only be obtained with a supercomputer (NEC

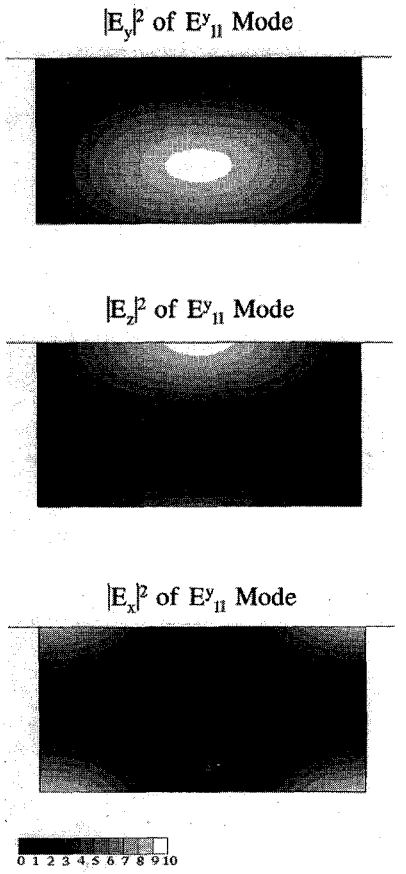


Fig. 4. Power distribution of the $E_{11}^y$ mode of the waveguide shown in Fig. 2. $|E_y|^2$ component (up), $|E_z|^2$ component (middle) and $|E_x|^2$ component (down). The amplitudes are normalized in order to give a maximum value of 10 for each component. Normalized frequency $v = 1$.

SX-2) after 35 seconds. Excellent convergence of magnitude and phase of the field has been verified. This is a very important property of the method since there are methods that, although achieve good convergence of the propagation constant, present very slow convergence of the field [10].

Next, the symmetrical coupler shown in Fig. 6 is examined. Coupling occurs between two pairs of modes. The first pair contains the even distributions $E_{\text{EVEN}}^x, E_{\text{EVEN}}^y$ while the second contains the odd ones $E_{\text{ODD}}^x, E_{\text{ODD}}^y$. The redundancy of the matrix is 73% and the calculation time of a single determinant is 14 seconds ($L = 9, N = 2$). In Fig. 6 are plotted the propagation constants of the four modes $Vs$ the spacing between the two channel waveguides. For large spacing the even and odd modes approach the surface modes of the single channel waveguide, marked with two little squares at $d/t = 1.5$. Also when $d/t \to 0$ the two waveguides become equivalent to a single one of double width. On the vertical axis at $d/t = 0$ four little squares mark the four lower modes $E_{11}^{x,y}, E_{21}^{x,y}$ of the single equivalent waveguide. We observe that the $E_{\text{EVEN}}^{x,y}$ modes tend to the $E_{11}^{x,y}$ modes, while the $E_{\text{ODD}}^{x,y}$ modes tend to the $E_{21}^{x,y}$ modes. From this figure it is concluded that it is possible to calculate the properties of a single waveguide by decomposing it into two (or more) smaller ones. If we do so, we can decrease the number of test functions ($L$) but the execution time will be $\tilde{}N^2$

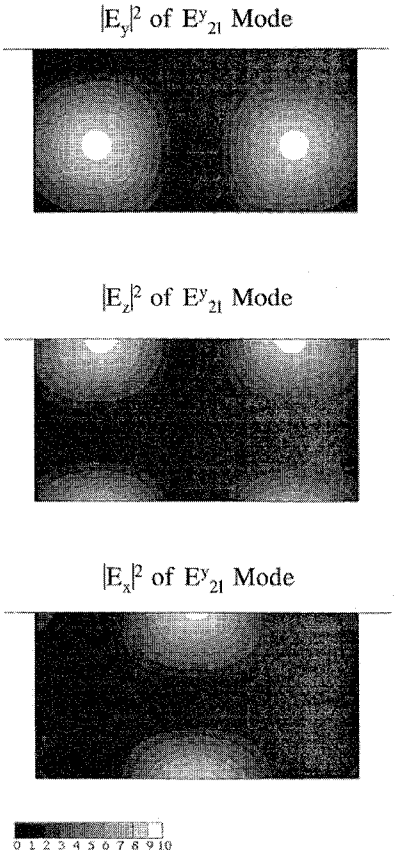


Fig. 5. Power distribution of the $E^y_{21}$ mode of the waveguide shown in Fig. 2. $|E_y|^2$ component (up), $|E_z|^2$ component (middle) and $|E_x|^2$ component (down). The amplitudes are normalized in order to give a maximum value of 10 for each component. Normalized frequency $v = 1$.

time larger. In Fig. 7 is shown the power distribution of the $E^x_{\text{EVEN}}$ and the $E^x_{\text{ODD}}$ mode when the separation distance is $d/t = 0.8$ and $d/t = 0.1$ (frequency $v = 1$). In Fig. 8 the evolution of the coupling phenomenon over a coupling length $L_c = (\pi/\beta_{\text{EVEN}} - \beta_{\text{ODD}})$ is plotted. The $E^y_{\text{EVEN}}$ and $E^y_{\text{ODD}}$ modes have been excited with equal amplitude. The five plots correspond to $z = 0, L_c/4, L_c/2, 3L_c/4, L_c$. At $z = 0$ the input power in the right waveguide is $-0.22$ dBm and in the left is $-13$ dBm. At $z = L_c$ the output power is $-13$ dBm and $-0.22$ dBm, respectively. The coupling length was found to be $L_c = 99.88\lambda_0$ ($\lambda_0 = 2\pi$). Although a 100% power transfer is achieved, there is always a noticeable amount of power remaining in one of the two waveguides at $z = 0, z = L_c$. This due to the small separation distance ($d/t = 0.1$).

Next the asymmetrical coupler shown in Fig. 9 is considered. Similar devices have been proposed for coupling a single-mode fiber to a thin-film waveguide [40]. Coupling occurs between the two lower pairs of modes which we will name $E^{x,y}_{\text{EVEN}}$ and $E^{x,y}_{\text{ODD}}$ although, strictly speaking, they are not characterized by complete (even and odd) symmetry with respect to the $X$ axis. The redundancy of the matrix is 59% and the calculation time of a single determinant is 20 seconds ($L = 9$). In Fig. 9 are plotted the propagation constants of the four lower modes $Vs$ the spacing between the two channel waveguides. For large spacing the even and odd modes approach the surface modes of the single rib

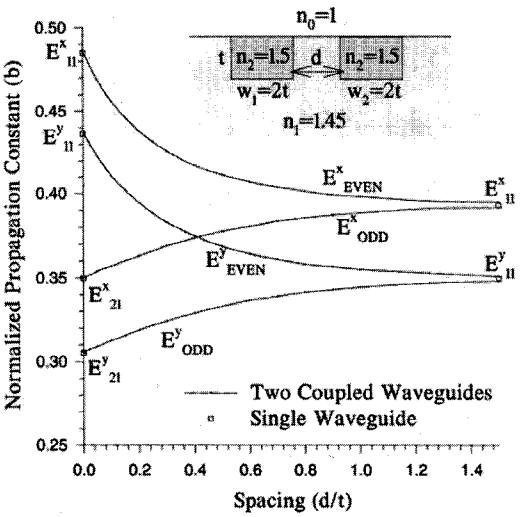


Fig. 6. Normalized propagation constants of a symmetrical coupler $Vs$ separation distance. $n_0 = 1, n_1 = 1.45, n_2 = 1.5, w/t = 2$. The surface modes of a single channel waveguide ($w/t = 2$) are marked with two little squares at $d/t = 1.5$. The four little squares on the vertical axis at $d/t = 0$ mark the four lower modes $E^{x,y}_{11}$, $E^{x,y}_{21}$ of a single waveguide with $w/t = 4$. Normalized frequency $v = 1$.

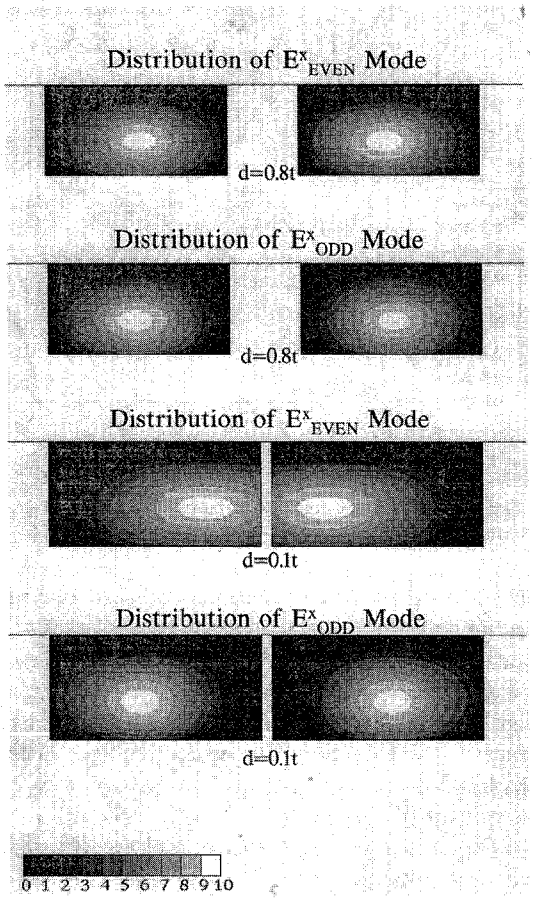


Fig. 7. Power distribution of even and odd modes of the symmetrical coupler shown in Fig. 6. Separation distance is $d/t = 0.8$ (up) and $d/t = 0.1$ (down). Normalized frequency $v = 1$.

waveguide ($A$) and the surface modes of the waveguide inside an infinite homogeneous substrate ($B$). The modes of the

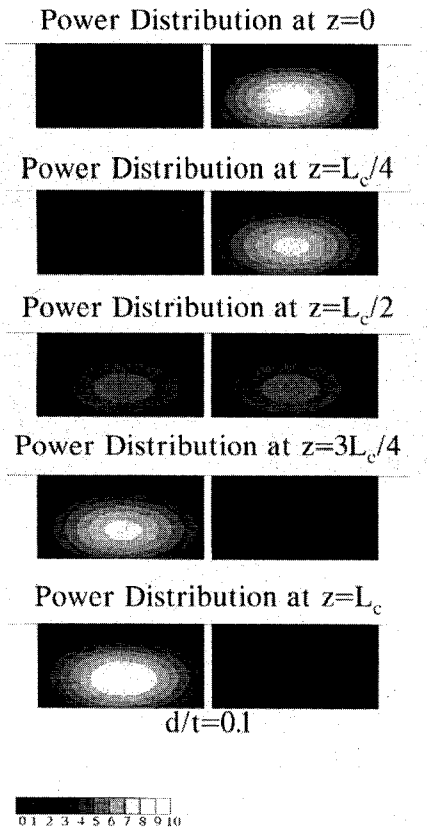


Fig. 8. Coupling phenomenon of the symmetrical coupler shown in Fig. 6 over a coupling length. Separation distance is $d/t = 0.1$. The five plots correspond to $z = 0, L_c/4, L_c/2, 3L_c/4, L_c$. Normalized frequency $v = 1$.

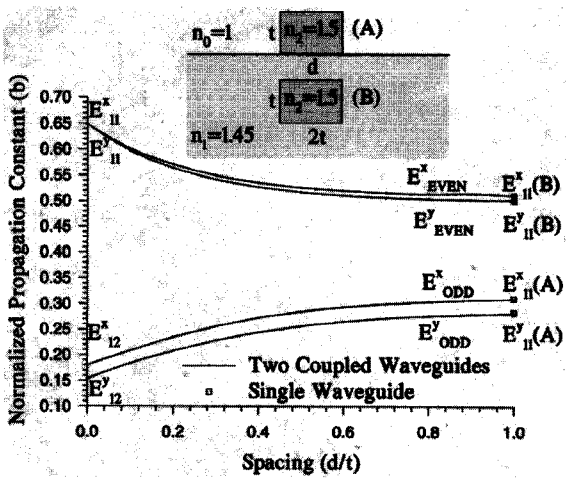


Fig. 9. Normalized propagation constants of an asymmetrical coupler $Vs$ separation distance. $n_0 = 1, n_1 = 1.45, n_2 = 1.5, w/t = 2$. Normalized frequency $v = 1$. The modes of the uncoupled waveguides $(A)$ and $(B)$ are marked with four little squares at $d/t = 1$.

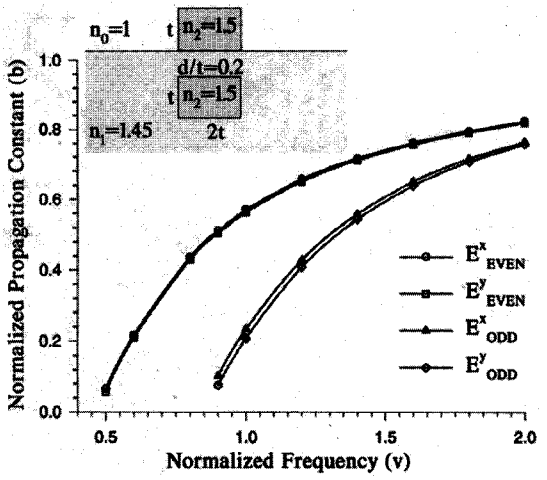


Fig. 10. The normalized propagation constants of the even and odd modes of the asymmetrical coupler $Vs$ normalized frequency. Separation distance is $d/t = 0.2$.

uncoupled waveguides $(A)$ and $(B)$ are marked with four little squares at $d/t = 1$. Also, when $d/t \to 0$ the two waveguides become equivalent to a single one, of aspect ratio $w/t = 1$ which is semi-embedded in the substrate. So the semi-embedded waveguide can be considered as a stack of a rib and a channel waveguide. The propagation constants of the four lower modes can be read on the vertical axis at $d/t = 0$. Fig. 10 depicts the dispersion curves of the four lower modes of the asymmetrical coupler, while Fig. 11 shows the convergence of the propagation constant of the $E^y_{\mathrm{ODD}}$ mode $Vs$ the number of test functions for $v = 1$. Once again the very rapid convergence of the method is verified.

In Fig. 12 the coupling phenomenon over a coupling length is plotted. The $E^x_{\mathrm{EVEN}}$ and $E^x_{\mathrm{ODD}}$ modes have been excited with equal amplitude. The separation distance is $d/t = 0.2$ and $v = 1$. The five plots correspond to $z = 0, L_c/4, L_c/2, 3L_c/4, L_c$. At $z = 0$ the input power in the upper waveguide is $-0.88$ dBm and in the lower is $-7.4$ dBm. At $z = L_c$ the output power is $-13.6$ dBm and $-0.55$ dBm, respectively. The coupling length was found to be $L_c = 29.67\lambda_0$ $(\lambda_0 = 2\pi)$. It is observed that a 100% power transfer is not possible.

As a final example the electric field of a channel waveguide having a trapezoidal cross section has been calculated. This waveguide is considered to be equivalent to a stack of ten smaller waveguides of rectangular cross section. The power distribution of the fundamental mode $|E_y|^2$ is shown in Fig. 13.

## V. Conclusion

An integral equation approach applied to the analysis of rectangular integrated optical waveguides has been presented. The embedding consists of a two layered isotropic and lossless medium. Galerkin's method is applied to solve the system of integral equations. A distinct difference of the present method is the use of entire domain test functions (plane waves) that are derived from a rigorous integral representation of the electric field. This results to a very rapid convergence and great economy in the required computer memory and CPU time. In the first example very good agreement with results of other methods is observed, thus establishing the validity of the present method. In the second and the third example coupling properties of symmetrical and asymmetrical structures have been investigated. Also it is shown how the same method can

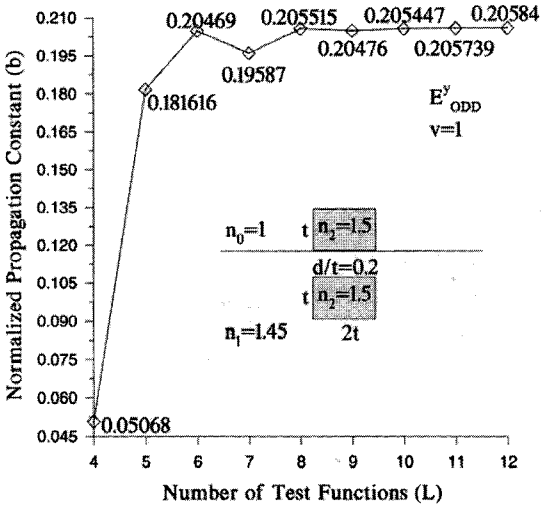


Fig. 11. Convergence of the normalized propagation constant of the $E^y_{ODD}$ mode. Normalized frequency $v = 1$.

be used to analyze more complicated cross sections like the semi-embedded waveguide and the waveguide of trapezoidal cross section.

## APPENDIX A

The dyadic functions $\underline{\overline{g}}_1, \underline{\overline{g}}_2$ can be found applying the boundary conditions at $y = 0$

$$\hat{y} \times (\underline{\overline{G}}_0 + \underline{\overline{G}}_1) = \hat{y} \times \underline{\overline{G}}_2 \tag{A1}$$

$$\hat{y} \times \nabla \times (\underline{\overline{G}}_0 + \underline{\overline{G}}_1) = \hat{y} \times \nabla \times \underline{\overline{G}}_2 \tag{A2}$$

and the Gauss condition for $\underline{\overline{G}}_1, \underline{\overline{G}}_2$:

$$\nabla \cdot \underline{\overline{G}}_1 = 0, \quad \nabla \cdot \underline{\overline{G}}_2 = 0. \tag{A3}$$

The above equations in combination with (5)–(17) give

$$\hat{y} \times (\underline{\overline{1}} k_n^2 - \underline{h}_0 \underline{h}_0) = \hat{y} \times (\underline{\overline{g}}_2 - \underline{\overline{g}}_1)\mu \tag{A4}$$

$$\hat{y} \times \underline{h}_0 \times \underline{\overline{1}} = \hat{y} \times (\underline{h}_2 \times \underline{\overline{g}}_2 - \underline{h}_1 \times \underline{\overline{g}}_1)\frac{\mu}{k_n^2} \tag{A5}$$

$$\underline{h}_1 \cdot \underline{\overline{g}}_1 = 0, \quad \underline{h}_1 \cdot \underline{\overline{g}}_1 = 0. \tag{A6}$$

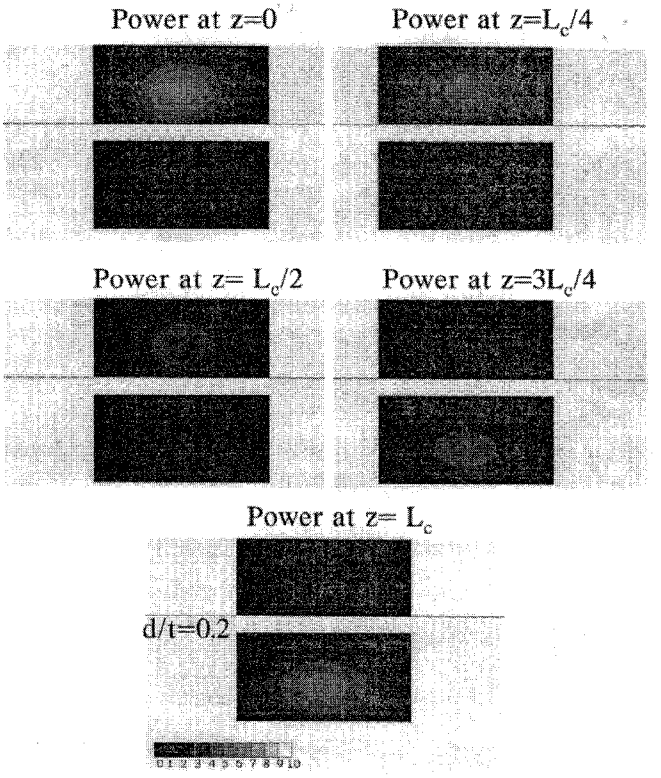


Fig. 12. Coupling phenomenon of the asymmetrical coupler shown in Fig. 9, over a coupling length. Separation distance is $d/t = 0.2$. The five plots correspond to $z = 0, L_c/4, L_c/2, 3L_c/4, L_c$. Normalized frequency $v = 1$.

The above equations form an algebraic system of eighteen equations. Its solution gives the unknown dyadic functions $\underline{\overline{g}}_1, \underline{\overline{g}}_2$

$$\underline{\overline{g}}_0(h_x, h_z, y', y - y') = \frac{1}{\mu}\begin{bmatrix} k_n^2 - h_x^2 & -jh_x\mu s & -h_x h_z \\ -jh_x\mu s & k_n^2 + \mu^2 & -jh_z\mu s \\ -h_x h_z & -jh_z\mu s & k_n^2 - h_z^2 \end{bmatrix} \tag{A7}$$

and (A8) and (A9), as shown at the bottom of the page.

$$\underline{\overline{g}}_1(h_x, h_z, y') = \begin{bmatrix} \dfrac{\mu a_5 + \mu'(h_x^2 - k_n^2)a_1}{a_3} & -\dfrac{jh_x a_9}{a_3} s_0 & -\dfrac{h_x h_z a_8}{a_3} \\ -\dfrac{jh_x a_2}{a_1} s_0 & -\dfrac{(k_n^2 + \mu^2)a_2}{\mu a_1} & -\dfrac{jh_z a_2}{a_1} s_0 \\ -\dfrac{h_x h_z a_8}{a_3} & -\dfrac{jh_z a_9}{a_3} s_0 & \dfrac{\mu a_7 + \mu'(h^2 z - k_n^2)a_1}{a_3} \end{bmatrix} \tag{A8}$$

$$\underline{\overline{g}}_2(h_x, h_z, y') = \begin{bmatrix} \dfrac{\mu a_5 - \mu(h_x^2 - k_n^2)a_1}{a_3} & -\dfrac{jh_x a_{10}}{a_3} s_0 & -\dfrac{2h_x h_z k_n^2}{a_1} \\ \dfrac{2j\mu h_x k_n^2}{a_1} s_0 & \dfrac{2(k_n^2 + \mu^2)k_n^2(y')}{a_1} & \dfrac{2j\mu h_z k_n^2}{a_1} s_0 \\ -\dfrac{2h_x h_z k_n^2}{a_1} & -\dfrac{jh_z a_{10}}{a_3} s_0 & \dfrac{\mu a_7 - \mu'(h_z^2 - k_n^2)a_1}{a_3} \end{bmatrix} \tag{A9}$$

$$\begin{aligned} a_1 &= \mu' k_n^2 + \mu k_n'^2 & a_2 &= \mu' k_n^2 - \mu k_n'^2 \\ a_3 &= \mu(\mu + \mu')a_1 & a_4 &= 2\mu k_n^2 + a_2 \\ a_5 &= k_n^2 a_1 - h_x^2 a_4 & a_6 &= k_n^2 a_1 - (k_n^2 + \mu^2)a_4 \\ a_7 &= k_n^2 a_1 - h_z^2 a_4 & a_8 &= \mu a_4 - \mu' a_1 \\ a_9 &= a_6 + \mu\mu' a_1 & a_{10} &= a_6 - \mu^2 a_1 \end{aligned}$$

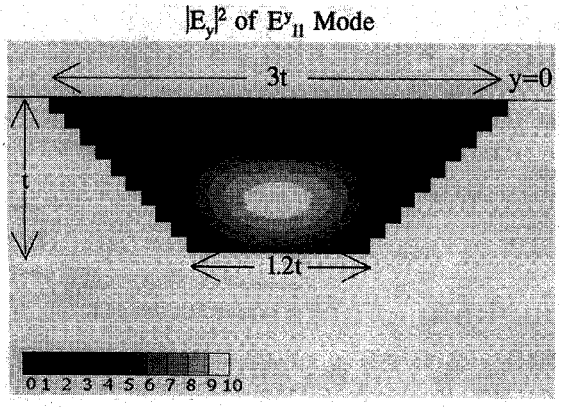


Fig. 13. Power distribution ($|E_y|^2$) of the $E^y_{11}$ mode of a channel waveguide with a trapezoidal cross section. Normalized frequency $v = 1, n_0 = 1, n_1 = 1.45, n_2 = 1.5$.

## APPENDIX B

Here is presented the calculation of the inner products (31). $t_0(X_1, X_2, C)$ denotes the following function:

$$t_0(X_1, X_2, C) = \frac{e^{X_2 C} - e^{X_1 C}}{C} \tag{B1}$$

$$\begin{aligned}\langle \underline{\overline{L}}^A_{im}[f_{l'}], f_l\rangle = \frac{k_2^2 - k_n^2(m)}{4\pi k_n^2(m)} \int_{-\infty}^{+\infty} dh_x \{ & t_0(X_1(m), X_2(m) \\ & j(k'_x - h_x)) t_0(X_1(i), X_2(i), j(h_x - k_x)) \\ & \cdot [\underline{\overline{A}} + t_0(Y_1(m), Y_2(m), (jk'_y - s_0\mu)) \\ & \cdot t_0(Y_1(i), Y_2(i), (-jk_y - s_0\mu)) \\ & \cdot \underline{\overline{g}}_1(h_x, \beta, y')]\}. \end{aligned} \tag{B2}$$

The scalar components $[\overline{\underline{A}}]_{\nu\xi}, \nu, \xi = 1, 2, 3$ of $\underline{\overline{A}}$ are given by

$$[\overline{\underline{A}}]_{\nu,\xi} = [\underline{\overline{g}}_0(h_x, \beta, |y - y'|)]_{\nu,\xi} [\underline{\overline{a}}]_{\nu,\xi}. \tag{B3}$$

The scalar components $[\underline{\overline{a}}]_{\nu,\xi}, \nu, \xi = 1, 2, 3$ of $\underline{\overline{a}}$ are the following integrals

$$\begin{aligned}[\underline{\overline{a}}]_{\nu\xi}(h_x) = & \int_{Y_1(i)}^{Y_2(i)} dy \int_{Y_1(m)}^{Y_2(m)} dy' \\ & \cdot e^{jk'_y y' - jk_y y - \mu|y - y'|} s_{\nu\xi}(y - y') \end{aligned} \tag{B4}$$

$$s_{\nu\xi}(y - y') = \begin{cases} 1 & \text{if } (\nu, \xi) = \{(1,1), (1,3), (2,2), \\ & \quad (3,1), (3,3)\} \\ \text{sign}(y - y') & \\ \quad \text{if } (\nu, \xi) = \{(1,2), (2,1), (2,3), (3,2)\}. \end{cases} \tag{B5}$$

The calculation of $[\underline{\overline{a}}]_{\nu\xi}$ depends on the relative position of the cross sections $S_i$ and $S_m$. For example if $Y_1(i) = Y_1(m)$ and $Y_2(i) = Y_2(m)$ then

$$\begin{aligned}[\underline{\overline{a}}]_{\nu\xi}(h_x) = & \frac{1}{jk'_y + \mu} [t_0(Y_1(i), Y_2(i), j(k'_y - k_y)) \\ & - t_0(Y_1(i), Y_2(i), (-jk_y - \mu)) e^{(jk'_y + \mu) Y_1(m)}] \\ & + \frac{1}{jk'_y - \mu} [t_0(Y_1(i), Y_2(i), (-jk_y + \mu)) \\ & \cdot e^{(jk'_y - \mu) Y_2(m)} - t_0(Y_1(i), Y_2(i), j(k'_y - k_y))] \\ & \cdot s_{\nu\xi}(-1) \end{aligned} \tag{B6}$$

similarly $[\underline{\overline{a}}]_{\nu\xi}(h_x)$ can be calculated for other relative positions of $S_i$ and $S_m$. The calculation of the following inner products is straightforward

$$\begin{aligned}\langle \underline{\overline{L}}^B_{im}[f_{l'}], f_l\rangle = & \frac{k_2^2 - k_n^2(m)}{4\pi k_n^2(m)} \int_{-\infty}^{+\infty} dh_x \\ & \cdot \{t_0(X_1(m), X_2(m), j(k'_x - h_x)) \\ & \cdot t_0(X_1(i), X_2(i), j(h_x - k_x)) \\ & \cdot t_0(Y_1(m), Y_2(m), (jk'_y - s_0\mu)) \\ & \cdot t_0(Y_1(i), Y_2(i), (-jk_y + s_0\mu')) \\ & \cdot \underline{\overline{g}}_2(h_x, \beta, y')\} \end{aligned} \tag{B7}$$

$$\begin{aligned}\langle f_{l'}, f_k\rangle = & t_0(X_1(i), X_2(i), j(k'_x - k_x)) \\ & \cdot t_0(Y_1(i), Y_2(i), j(k'_y - k_y)). \end{aligned} \tag{B8}$$

## REFERENCES


[1] E. A. J. Marcatili, "Dielectric rectangular waveguide and directional coupler for integrated optics," *Bell Syst. Tech. J.*, vol. 48, no. 9, pp. 2071–2102, Sept. 1969.

[2] R. M. Knox and P. P. Toulios, "Integrated circuits for the millimeter through optical frequency region," *Proc. Symp. Submillimeter Waves*, New York, Mar. 1970, pp. 497–519.

[3] W. V. McLevige, T. Itoh, and R. Mittra, "New waveguide structures for millimeter-wave and optical integrated circuits," *IEEE Trans. Microwave Theory Tech.*, vol. MTT-23, no. 10, pp. 788–794, Oct. 1975.

[4] T. Trinh and R. Mittra, "Coupling characteristics of planar dielectric waveguides of rectangular cross section," *IEEE Trans. Microwave Theory Tech.*, vol. MTT-29, no. 9, pp. 875–880, Sept. 1981.

[5] S. M. Saad, "Review of numerical methods for the analysis of arbitrarily-shaped microwave and optical dielectric waveguides," *IEEE Trans. Microwave Theory Tech.*, vol. MTT-33, no. 10, pp 894–899, Oct. 1985.

[6] J. E. Goell, "A circular-harmonic computer analysis of rectangular dielectric waveguides," *Bell Syst. Tech. J.*, vol. 48, pp. 2133–2160, Sept. 1969.

[7] S. T. Peng and A. A. Oliner, "Guidance and leakage properties of a class of open waveguides: Part I-Mathematical formulations," *IEEE Trans. Microwave Theory Tech.*, vol. MTT-29, pp. 843–855, Sept. 1981.

[8] A. A. Oliner and S. T. Peng, "Guidance and leakage properties of a class of open waveguides: Part II-New physical effects," *IEEE Trans. Microwave Theory Tech.*, vol. MTT-29, pp. 855–869, Sept. 1981.

[9] U. Crombach, "Analysis of single and coupled rectangular dielectric waveguides," *IEEE Trans. Microwave Theory Tech.*, vol. MTT-29, no. 9, pp. 870–874, Sept. 1981.

[10] K. Yasuura, K. Shimohara and T. Miyamoto, "Numerical analysis of a thin film waveguide by mode-matching method," *J. Opt. Soc. Am.*, vol. 70, no. 2, pp. 183–191, Feb. 1980.

[11] H. Kubo and K. Yasumoto, "Numerical Analysis of Three-Parallel Embedded Optical Waveguides," *J. Lightwave Technol.*, vol. 7, no. 12, pp. 1294–1930, Dec. 1989.

[12] Q. H. Liu and W. C. Chew, "Analysis of complex rectangular dielectric waveguides," *J. Electromagnetic Waves Applicat.*, vol. 5, no. 3, pp. 253–256, 1991.

[13] M. Ikeuchi, H. Sawami, and H. N. Ki, "Analysis of open-type dielectric waveguides by the finite-element iterative method," *IEEE Trans. Microwave Theory Tech.*, vol. MTT-29, pp. 234–239, Mar. 1981.

[14] N. Mabaya, P. E. Legasse, and P. Vandenbulcke, "Finite-element analysis of optical waveguides," *IEEE Trans. Microwave Theory Tech.*, vol. MTT-29, pp. 600–605, June 1981.

[15] B. M. A. Rahman and J. B. Davies, "Penalty function improvement of waveguide solution by finite elements," *IEEE Trans. Microwave Theory Tech.*, vol. MTT-32, no. 8, pp, 922–928, Aug. 1984.

[16] ——, "Finite-element solution of integrated optical waveguides," *J. Lightwave Technol.*, vol. LT-2, no. 5, pp. 682–693, Oct. 1984.

[17] ——, "Finite-element analysis of optical and waveguide problems," *IEEE Trans. Microwave Theory Tech.*, vol. MTT-32, pp. 20–28, Jan. 1984.

[18] M. Koshiba, K. Hayata, and M. Suzuki, "Improved finite-element formulation in terms of the magnetic field vector for dielectric waveguides," *IEEE Trans. Microwave Theory Tech.*, vol. MTT-33, pp. 227–233, Mar. 1985.

[19] ——, "Finite-element formulation in terms of the electric field vector for electromagnetic waveguide problems," *IEEE Trans. Microwave Theory Tech.*, vol. MTT-33, pp. 900–905, 1985.
[20] K. Bierwirth, N. Schulz, and F. Arndt, "Finite-difference analysis of rectangular dielectric waveguide structures," *IEEE Trans. Microwave Theory Tech.*, vol. MTT-34, pp. 1104–1114, 1986.
[21] A. T. Galick, T. Kerkhoven, and U. Ravaioli, "Iterative solution of the eigenvalue problem for a dielectric waveguide," *IEEE Trans. Microwave Theory Tech.*, vol. 40, no. 4, pp. 699–705, Apr. 1992.
[22] J. S. Bagby, D. P. Nyquist, and B C. Drachman, "Integral formulation for analysis of integrated dielectric waveguides," *IEEE Trans. Microwave Theory Tech.*, vol. MTT-33, no. 10, pp. 906–915, Oct. 1985.
[23] J. S. Bagby and D. P. Nyquist, "Dyadic Green's functions for integrated electronics optical circuits," *IEEE Trans. Microwave Theory Tech.*, vol. MTT-35, pp. 206–210, Feb 1987.
[24] E. W. Kolk, N. H. G. Baken, and H. Blok, "Domain integral equation analysis of integrated optical channel and ridge waveguides in stratified media," *IEEE Trans. Microwave Theory Tech.*, vol. 38, no. 1, pp. 78–85, Jan. 1990.
[25] J.-F. Kiang, S. M. Ali, and J. A. Kong, "Integral equation to the guidance and leakage properties of coupled dielectric strip waveguides," *IEEE Trans. Microwave Theory Tech.*, vol. 38, no. 2, pp. 193–203, Feb. 1990.
[26] N. H. G. Baken, M. B. J. Diemeer, J. M. Van Splunter, and H. Blok, "Computational modeling of diffused channel waveguides using a domain integral equation," *J. Lightwave Technol.*, vol. 8, no. 4, pp. 576–586, Apr. 1990.
[27] H. J. M. Bastiansen, N. H. G. Baken, and H. Blok, "Domain-integral analysis of channel waveguides in anisotropic multilayered media," *IEEE Trans. Microwave Theory Tech.*, vol. 40, no 10, pp. 1918–1926, Oct. 1992.
[28] P. Cottis and N. Uzunoglu, "Integral equation approach for the analysis of anisotropic channel waveguides," *J Opt. Soc. Am A*, vol. 8, no. 4, pp. 608–614, Apr. 1991.
[29] C. C. Su, "A surface integral equations method for homogeneous optical fibers and coupled image lines of arbitrary cross sections," *IEEE Trans. Microwave Theory Tech.*, vol. MTT-34, pp. 1140–1146, Sept. 1986.
[30] J. Van Bladel, *Singular Electromagnetic Fields and Sources*. London: Oxford Univ. Press, 1991.
[31] S W. Lee, J. Boersma, C. L. Law, and G. A. Deschamps, "Singularity in Green's function and its numerical evaluation," *IEEE Trans. Antennas Propagat.*, vol. AP–28, pp. 311–317, 1980.
[32] P. M. Morse and H. Fesbach, *Methods of Theoretical Physics*, Parts I and II. New York: McGraw-Hill, 1953.
[33] M. S. Viola and D. P. Nyquist, "An observation on the Sommerfeld-Integral representation of the electric dyadic Green's function for layered media," *IEEE Trans. Microwave Theory Tech.*, vol. MTT-36, no. 8, pp. 1289–1292, 1988.
[34] A. D. Yaghjian, "Electric dyadic Green's functions in the source region," *Proc. IEEE*, vol. 68, pp. 248–263, 1980.
[35] J. J. H. Wang, "A unified consistent view on the singularities of the electric dyadic Green's function in the source region," *IEEE Trans. Antennas Propagat.*, vol. AP-30, pp. 463–468, 1982.
[36] V. S Vladimirov, *Equations of Mathematical Physics* Moscow: Mir, 1984, English translation.
[37] R. F. Harrington, "Matrix methods for field problems," *Proc. IEEE*, vol. 55, pp. 136–149, 1967.
[38] C. A. J. Fletcher, *Computational Galerkin Methods*. New York: Springer-Verlag, 1984.
[39] M. Abramowitz and I. A. Stegun, *Handbook of Mathematical Functions*. New York: Dover, 1972, ch. 25, p. 887.
[40] Y. Cai and T. Mizumoto, "An effective method for coupling single-mode fiber to thin-film waveguide" *Journal of Lightwave Technology*, vol. 9, no. 5, pp. 577–583, May 1991.

**Spyridon J. Polychronopoulos** was born in Athens, Greece, in 1965. He received the Diploma degree in electrical engineering from the National Technical University of Athens (NTUA) in 1987, the M.Sc degree from the University of Manchester Institute of Science and Technology, UK, in 1988, and the Ph.D. degree from the Department of Electrical and Computer Engineering of NTUA in 1993.

His research activities include analytical and numerical methods in electromagnetic waves and guidance phenomena in microwave circuits.

**Nikolaos K. Uzunoglu** (M'82) was born in Constantinopole in 1951. He received the B.Sc degree in electronics from the Technical University of Istanbul in 1973, and the M.Sc. and Ph.D. degrees in 1974 and 1976, respectively, from the University of Essex, UK

He worked from 1977 to 1984 as a Research Scientist at the Office of Research and Technology of the Hellenic Navy. In 1984, he was elected Associate Professor at the Department of Electrical Engineering, National Technical University of Athens (NTUA), and in 1987 he was promoted to Professor. In 1986, he was elected Vice-Chairman of the Department of Electrical Engineering, NTUA, and in 1988 he was elected Chairman of the same department. He was reelected as Chairman in 1992. In 1991, he was elected and appointed Director of the Institute of Communications and Computer Systems, an independent research establishment associated with NTUA. His research interests include electromagnetic scattering, radiation phenomena, propagation of electromagnetic waves in atmosphere, medical applications of electromagnetic waves, fiber optics telecommunications, and high-speed circuits operating at Gb/s rates. He has 100 publications in refereed international journals, and he published three books in Greek on microwaves, fiber optics telecommunications, and radar systems.

Dr. Uzunoglu received the International G. Marconi award in Telecommunications in 1981. Since 1988, he has been the National Representative of Greece to the COST, Technical Telecommunications Committee, actively participating in several COST projects. Further, he has been Project Manager in several RACE, ESPRIT, and national research and development projects in the fields of telecommunications and biomedical engineering.